

# SCIENTIFIC REPORTS



OPEN

## Physiological and transcriptomic analyses reveal mechanistic insight into the adaptation of marine *Bacillus subtilis* C01 to alumina nanoparticles

Received: 17 March 2016

Accepted: 24 June 2016

Published: 21 July 2016

Dashuai Mu<sup>1,2</sup>, Xiuxia Yu<sup>2</sup>, Zhenxing Xu<sup>2</sup>, Zongjun Du<sup>1,2</sup> & Guanjun Chen<sup>1,2</sup>

An increasing number of studies have investigated the effects of nanoparticles (NPs) on microbial systems; however, few existing reports have focused on the defense mechanisms of bacteria against NPs. Whether secondary metabolism biosynthesis is a response to NP stress and contributes to the adaptation of bacteria to NPs is unclear. Here, a significant induction in the surfactin production and biofilm formation were detected by adding Al<sub>2</sub>O<sub>3</sub> NPs to the *B. subtilis* fermentation broth. Physiological analysis showed that Al<sub>2</sub>O<sub>3</sub> NP stress could also affect the cell and colony morphogenesis and inhibit the motility and sporulation. Exogenously adding commercial surfactin restored the swarming motility. Additionally, a suite of toxicity assays analyzing membrane damage, cellular ROS generation, electron transport activity and membrane potential was used to determine the molecular mechanisms of toxicity of Al<sub>2</sub>O<sub>3</sub> NPs. Furthermore, whole transcriptomic analysis was used to elucidate the mechanisms of *B. subtilis* adaptation to Al<sub>2</sub>O<sub>3</sub> NPs. These results revealed several mechanisms by which marine *B. subtilis* C01 adapt to Al<sub>2</sub>O<sub>3</sub> NPs. Additionally, this study broadens the applications of nanomaterials and describes the important effects on secondary metabolism and multicellularity regulation by using Al<sub>2</sub>O<sub>3</sub> NPs or other nano-products.

There has been a quantum increase in the use of nanoparticles (NPs) in many spheres of life. The physical and chemical properties of NPs can vary significantly from those of their bulk counterparts<sup>1</sup>. Nanoparticles are being considered for use in combating diseases such as cancer<sup>2</sup>, or fighting bacterial pathogens<sup>3</sup>. Beyond biomedical applications, there are established uses of nanoparticles for industrial applications and commercial products.

The increased presence of NPs in environment necessitates a basic understanding of their interactions with biomolecules and biological systems. The toxic effects of nanoparticles, termed “nanotoxicity,” are increasingly evident. Previous studies in animals and cell culture have amply demonstrated loss of cell viability, tissue damage and inflammatory reactions<sup>4</sup>.

Recently, an increasing number of studies have investigated the effects of NPs on microbial systems. The antimicrobial properties of NPs are attractive for their efficacy and low cost, and they have been demonstrated against a wide range of microorganisms, including drug-resistant strains<sup>5</sup>. Nanoparticles have been shown to inhibit growth of *Escherichia coli*, *Pseudomonas aeruginosa*, *Klebsiella pneumoniae*, and several other multidrug-resistant microorganisms<sup>6</sup>. Zinc oxide and magnesium oxide NPs were found to exert significant growth inhibitory effects, which were related to membrane damage and oxidative stress responses in *Escherichia coli*<sup>7</sup>. Nitric-oxide-releasing NPs are able to change the structure of the bacterial membrane and produce reactive nitrogen species (RNS), which lead to modification of essential bacterial proteins<sup>8</sup>. In contrast, Ag NPs and Cu NPs prevent biofilm formation, induce ROS generation, and cause DNA damage in common pathogens, such as *E. coli*<sup>9,10</sup>. It should be mentioned that Al<sub>2</sub>O<sub>3</sub> NPs could attach to the cell wall and travel into the cytoplasm of *E. coli*, where they exert toxic effects<sup>11,12</sup>. Also, Al<sub>2</sub>O<sub>3</sub> NPs could cause the cell wall damage and lipid peroxidation

<sup>1</sup>State Key Laboratory of Microbial Technology, Shandong University, Jinan 250100, PR China. <sup>2</sup>College of Marine Science, Shandong University (Weihai), Weihai 264209, PR China. Correspondence and requests for materials should be addressed to Z.D. (email: duzongjun@sdu.edu.cn) or G.C. (email: guanjun@sdu.edu.cn)

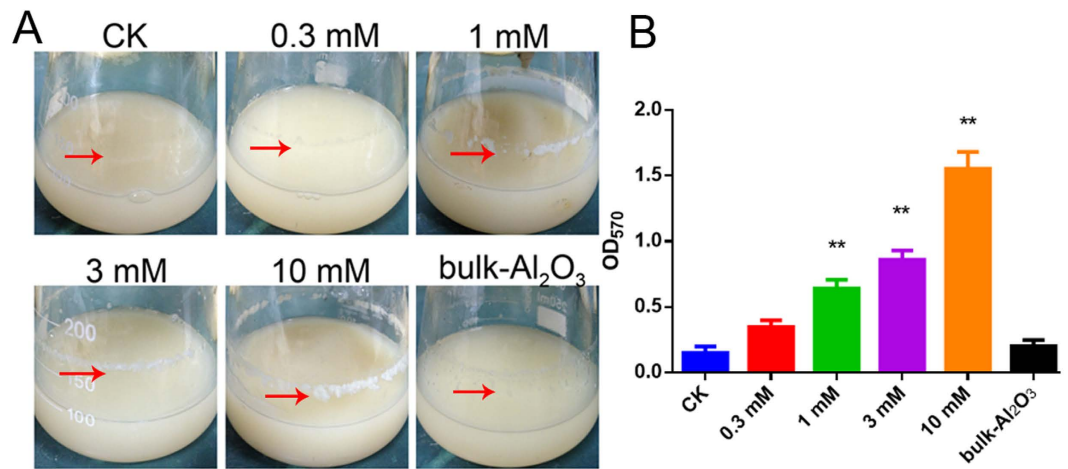


**Figure 1. Phenotypic analysis and quantification of biofilm formation.** CK means control, 0.3 mM, 1 mM, 3 mM, 10 mM mean various concentration of Al<sub>2</sub>O<sub>3</sub> NPs, bulk-Al<sub>2</sub>O<sub>3</sub> means 10 mM bulk-Al<sub>2</sub>O<sub>3</sub>. (A) Phenotypic analysis of biofilm formation on the flask, the fermentation broth was 100 ml in the 250 ml flask, treated with different concentration of Al<sub>2</sub>O<sub>3</sub> NPs for shaken culturing 60 h. The white cycles on the flask was the biofilms; (B) Quantification of biofilm by staining with crystal violet (\*\**p* < 0.01, *n* = 3).

then caused a decrease in cell viability of *Bacillus licheniformis*<sup>12</sup>. However, these reports mainly focused on the antibacterial properties of NPs, whether or how microorganism adapt to NP stress remains unclear.

*Bacillus* species as biological control agents are receiving increased attention because of their ability to produce various antimicrobial substances. Additionally, these species are commonly used as a model Gram-positive strain for drug-resistance analysis. As a result, the antimicrobial effects of NPs have been explored with *B. subtilis*. Toxicity of Ag and ZnO NPs towards *B. subtilis* is significantly less due to the presence of a thicker peptidoglycan layer<sup>13</sup>. Previous studies have addressed the role of a limited sub-set of *B. subtilis* genes in response to Al<sub>2</sub>O<sub>3</sub> NPs but the potentially pan-metabolic action of Al<sub>2</sub>O<sub>3</sub> NPs on cells alludes to large-scale genetic regulation<sup>14</sup>. For Al<sub>2</sub>O<sub>3</sub> NPs, the toxic mechanism may be enhanced by association of the nanoparticle and bacterial surface and subsequent cell wall binding followed by the enhancement of permeability<sup>15</sup>, however, how *B. subtilis* adapt to the Al<sub>2</sub>O<sub>3</sub> NPs remains unknown. In our earlier study, we reported that Al<sub>2</sub>O<sub>3</sub> NPs can be used as effective flocculants for flocculating *B. subtilis*, and the possible attachment mechanisms of Al<sub>2</sub>O<sub>3</sub> NPs to the *B. subtilis* surface may be electrostatic<sup>16</sup>. Whether this electrostatic attachment could affect or change the physiological phenotype and development or affect secondary metabolism remained unclear.

Nearly 30 years ago, James A. Shapiro proposed multicellularity as a general bacterial trait<sup>17</sup>, and *B. subtilis* is now one of the classical and best-studied bacterial species<sup>18</sup>. Given that Al<sub>2</sub>O<sub>3</sub> NPs damage the bacterial cell wall and increase permeability, resulting in growth inhibition, we wondered whether or how Al<sub>2</sub>O<sub>3</sub> NPs affect multicellularity and secondary metabolism of *B. subtilis*, and how *B. subtilis* adapt to a certain concentration of Al<sub>2</sub>O<sub>3</sub> NPs. To test this aim, various concentrations of Al<sub>2</sub>O<sub>3</sub> NPs were added during the culturing and fermentation of surfactin of *B. subtilis*. We noted a significant induction in the surfactin production and biofilm formation by adding Al<sub>2</sub>O<sub>3</sub> NPs in the fermentation broth. Al<sub>2</sub>O<sub>3</sub> NPs also influenced the motility, colony morphology, and sporulation. Furthermore, a suite of toxicity assays testing membrane damage, cellular ROS generation, electron transport activity and membrane potential was used to determine the molecular mechanisms of toxicity of Al<sub>2</sub>O<sub>3</sub> NPs compared to their micro-sized analogues. To capture the overall genetic response to Al<sub>2</sub>O<sub>3</sub> NPs and bulk-Al<sub>2</sub>O<sub>3</sub> and to explore the mechanism of adaption to Al<sub>2</sub>O<sub>3</sub> NPs, whole transcriptomic analysis was used. These results reveal a new mechanism of how marine *B. subtilis* C01 adapted to alumina NPs. Additionally, this study broadens the potential applications of nanomaterials and has important implications for secondary metabolism and multicellularity regulation by using Al<sub>2</sub>O<sub>3</sub> NPs and for exploring other nano-products useful in product fermentation or bio-medical applications.

## Results

**Effect of Al<sub>2</sub>O<sub>3</sub> NPs on biofilm formation.** In our previous study, it was reported that Al<sub>2</sub>O<sub>3</sub> NPs can be used as effective flocculants for flocculation of *B. subtilis*<sup>16</sup>. During the flocculation by using different concentrations of 40 nm Al<sub>2</sub>O<sub>3</sub> NPs, which have been characterised in our earlier study<sup>15</sup>, biofilm formation was also found to be influenced to varying degrees (Fig. 1A). After treating *B. subtilis* with 0.3, 1, 3, or 10 mM of 40 nm Al<sub>2</sub>O<sub>3</sub> NPs and continuing shake culturing for 60 h, biofilm formation of *B. subtilis* was enhanced as the concentration of Al<sub>2</sub>O<sub>3</sub> NPs increased, although high concentrations of Al<sub>2</sub>O<sub>3</sub> NPs could inhibit the growth of planktonic cells (Figs 1B and 2A). The quantitative analysis of biofilm formation using crystal violet was similar to the phenotypic analysis (Fig. 1A,B).

However, it remained unknown whether Al<sub>2</sub>O<sub>3</sub> NPs had the same effect on *B. subtilis* when stationary culturing. To test this, biofilm formation was monitored when Al<sub>2</sub>O<sub>3</sub> NPs were added in the liquid fermentation broth followed by stationary culturing. In contrast to shake culturing, Al<sub>2</sub>O<sub>3</sub> NPs prevented biofilm formation

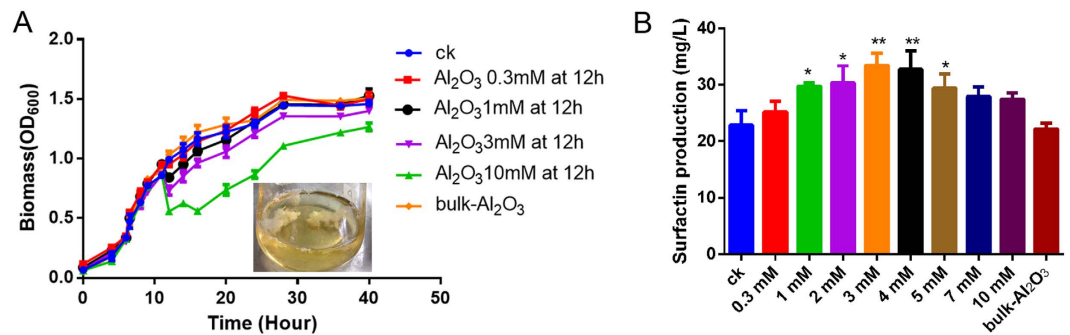


**Figure 2.** Al<sub>2</sub>O<sub>3</sub> NPs enhances the surfactin production. (A) Time course of *B. subtilis* growth and the dosage of Al<sub>2</sub>O<sub>3</sub> NPs treatment on fermentation; (B) Surfactin production of *B. subtilis* treated with various concentration of Al<sub>2</sub>O<sub>3</sub> NPs, Methanolic extracts containing surfactin from cell-free supernatants of various treatment were fractionated by RP-HPLC analysis and detection at 214 nm. CK means control, 0.3 mM, 1 mM, 2 mM, 3 mM, 4 mM, 5 mM, 7 mM, 10 mM mean various concentration of Al<sub>2</sub>O<sub>3</sub> NPs, bulk-Al<sub>2</sub>O<sub>3</sub> means 10 mM bulk-Al<sub>2</sub>O<sub>3</sub> (\*P < 0.05, \*\*P < 0.01, n = 3).

in stationary culturing (Fig. S1), which was probably due to the flocculation effect of Al<sub>2</sub>O<sub>3</sub> NPs (Fig. 2A), which resulted in the restriction of motility. However, the exact mechanisms need to be determined in subsequent studies. Taken together, Al<sub>2</sub>O<sub>3</sub> NPs appear to be involved in the regulation of biofilm formation.

**Effect of Al<sub>2</sub>O<sub>3</sub> NPs on surfactin production.** Surfactin was quantified using HPLC to determine whether the surfactin production changed after the flocculation by Al<sub>2</sub>O<sub>3</sub> NPs. The results showed 3 mM Al<sub>2</sub>O<sub>3</sub> NPs could induce the surfactin production (Fig. 2B). High concentrations of Al<sub>2</sub>O<sub>3</sub> NPs inhibit the growth of microorganisms<sup>15</sup>; therefore, organisms require a suitable concentration and induction time of Al<sub>2</sub>O<sub>3</sub> NPs to adjust the growth and metabolism. To evaluate this effect, the concentration of Al<sub>2</sub>O<sub>3</sub> NPs was varied from 0 to 10 mM. Surfactin accumulation increased with increasing concentrations of Al<sub>2</sub>O<sub>3</sub> NPs until a limiting maximum concentration (3 mM or 4 mM) was reached (Fig. 2A,B), and growth was reduced when the dosage was 10 mM. In response to varying Al<sub>2</sub>O<sub>3</sub> NPs induction times (0–72 h), the highest yield (33.5 mg/L) was at 12 h (Fig. S2). It is well known that NP size holds an intriguing role on its physico-chemical property and subsequent effect on microbial system. In our study, we found that 3 mM small size (40 nm) of Al<sub>2</sub>O<sub>3</sub> NPs could induce more surfactin production compared with that induced by large size (110 nm and 280 nm) of Al<sub>2</sub>O<sub>3</sub> NPs (data not shown). As a result, the addition of 3 mM Al<sub>2</sub>O<sub>3</sub> NPs (40 nm) at 12 h to the fermentation media is the suggested treatment condition for further physiological study.

**Al<sub>2</sub>O<sub>3</sub> NPs influence morphogenesis and motility.** To evaluate the effect of Al<sub>2</sub>O<sub>3</sub> NPs on *B. subtilis* C01 morphogenesis, C01 was grown on 2216E medium with or without 3 mM Al<sub>2</sub>O<sub>3</sub> NPs. As shown in Fig. 3, C01 control populations on the agar medium develop colonies with robust morphology. However, the robustness of colony morphology was dramatically diminished on the 3 mM Al<sub>2</sub>O<sub>3</sub> NP-containing agar medium. Colonies grown on the bulk-Al<sub>2</sub>O<sub>3</sub>-containing agar medium were similar to those on control agar medium (Fig. 3).

To investigate the effect of Al<sub>2</sub>O<sub>3</sub> NPs on surface motility, bacteria were spotted onto the centers of 2216E soft agar swarm plates (0.3% of agar in the 2216E medium with or without 3 mM Al<sub>2</sub>O<sub>3</sub> NPs). Within 6–8 h of incubation, the bacteria formed a colony of 2–4 cm diameter in control swarm plates (Fig. 3). However, the presence of 3 mM Al<sub>2</sub>O<sub>3</sub> NPs significantly altered the motility of bacterial cells compared to control in which no Al<sub>2</sub>O<sub>3</sub> NPs were present (Fig. 3). The results showed that Al<sub>2</sub>O<sub>3</sub> NPs could influence the morphogenesis and motility due to the nano-size of this particle, as bulk-Al<sub>2</sub>O<sub>3</sub> could not influence these phenotypes.

To determine whether Al<sub>2</sub>O<sub>3</sub> NPs could affect the flagella, we carried out microscopic studies of cells collected from the control fermentation broth and broth treated by 3 mM Al<sub>2</sub>O<sub>3</sub> NPs (Fig. 3). TEM results showed that cells from the control or bulk-Al<sub>2</sub>O<sub>3</sub>-added fermentation broth have a number of peritrichous flagella. However, under Al<sub>2</sub>O<sub>3</sub> NPs treatment, Al<sub>2</sub>O<sub>3</sub> NPs could attach to the membrane and cause the flagellar damage, because cells from such treatment showed flagella missing or agglomerate flagella, and floccules was found attached to the cells (Fig. 3). In addition, the cell morphology was significantly different in the presence and absence of Al<sub>2</sub>O<sub>3</sub> NPs, and Al<sub>2</sub>O<sub>3</sub> NPs could attach to the cell membrane (Fig. 3).

A consensus has emerged that swarming motility by *B. subtilis* requires or must be facilitated by the production of the lipopeptide surfactin<sup>19,20</sup>. Figure 3 shows that exogenously adding commercial surfactin in 2216E agar media could significantly restore the swarming motility and cell morphology compared to the Al<sub>2</sub>O<sub>3</sub> NPs treatment. However, in the fermentation broth, surfactin did not reduce the flagellar damage, as the flagella of the cells in such treatment was also missing or agglomerate according to the TEM analysis (Fig. 3). Taken together, a relatively high surfactin production could restore and enhance swarming motility under Al<sub>2</sub>O<sub>3</sub> NP stress, as exogenously adding commercial surfactin in Al<sub>2</sub>O<sub>3</sub> NP treatment media could enhance the motility (Fig. 3).

**The mechanisms of toxicity for Al<sub>2</sub>O<sub>3</sub> NPs on *B. subtilis*.** To elucidate the mechanisms of toxicity for the Al<sub>2</sub>O<sub>3</sub> NPs, a suite of assays measuring membrane potential, membrane damage, cellular ROS generation, and electron transport activity was employed in *B. subtilis* (see the Supporting Information for methods).

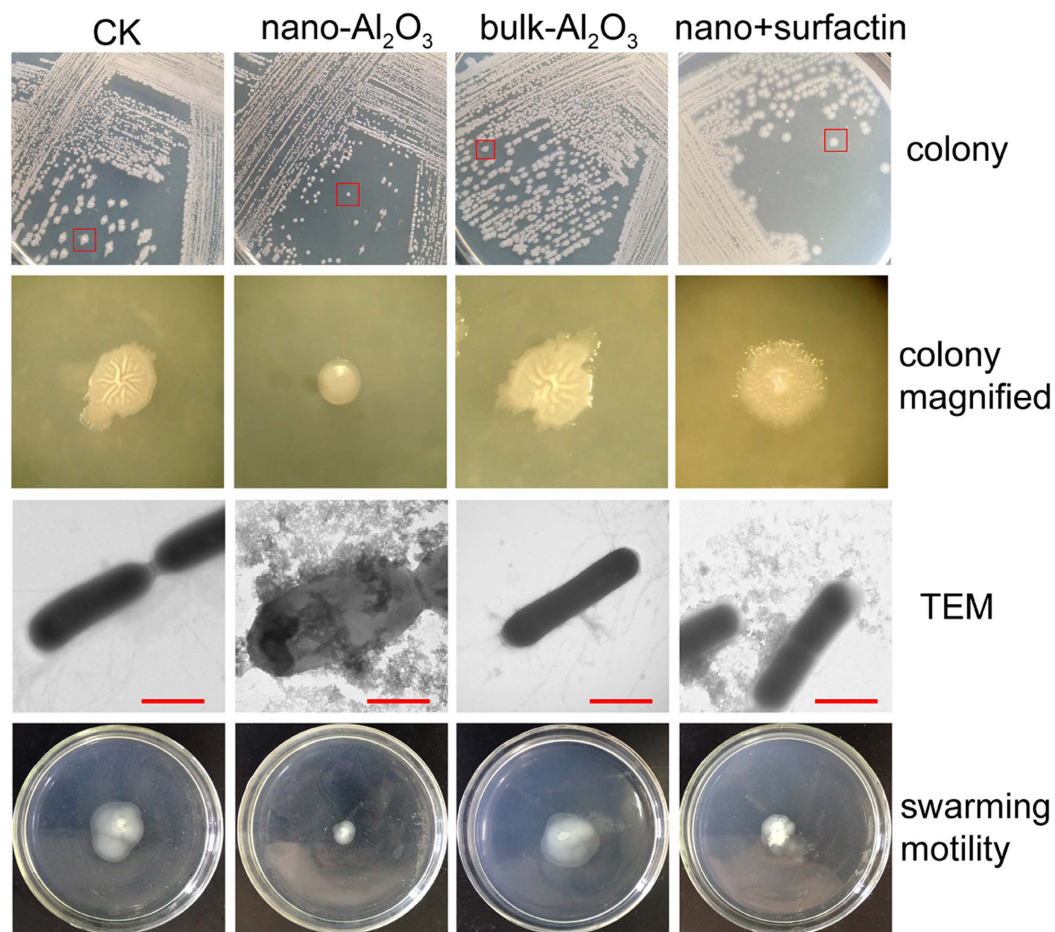


**Figure 3. Influence of  $\text{Al}_2\text{O}_3$  NP stress on the colony morphogenesis and motility of *B. subtilis* C01.** CK indicates control treatment, nano- $\text{Al}_2\text{O}_3$  indicates 3 mM  $\text{Al}_2\text{O}_3$  NPs were added in the 2216E agar plate or fermentation at 12 h, bulk-  $\text{Al}_2\text{O}_3$  indicates 3 mM bulk- $\text{Al}_2\text{O}_3$  treatment, nano+surfactin indicates both 3 mM  $\text{Al}_2\text{O}_3$  NPs and 20  $\mu\text{M}$  commercial surfactin were added to the culture. Colony indicates the colony of C01 grew on a different plate, the red box indicates the colony selected for colony magnified analysis; TEM shows the cells with different treatment, red bar = 500 nm; swarming motility indicates growth of *B. subtilis* strains on media with 0.3% agar and different treatments. Bacteria were centrally inoculated onto the soft plates.

The outcomes of these assays are shown in Fig. S3.  $\text{Al}_2\text{O}_3$  NPs resulted in significant membrane damage and an increase in ROS generation at 3 mM and 10 mM concentrations (Fig. S3A,B), while bulk- $\text{Al}_2\text{O}_3$  did not result in membrane damage and ROS generation even by using 10 mM. This observation strongly agrees with the TEM analysis (Fig. 3) and growth inhibition results. Conversely, no disruption of membrane potential was observed in *B. subtilis* treated with either  $\text{Al}_2\text{O}_3$  NPs or bulk- $\text{Al}_2\text{O}_3$  (Fig. S3C). Additionally, electron transport activity was not influenced by  $\text{Al}_2\text{O}_3$  NPs and bulk- $\text{Al}_2\text{O}_3$  (Fig. S3D). These results highlight important mechanistic pathways of toxicity for  $\text{Al}_2\text{O}_3$  NPs.

**Two-component signal systems and membrane proteins response to  $\text{Al}_2\text{O}_3$  NP treatment.** For genes involved in the response of  $\text{Al}_2\text{O}_3$  NPs stress screening, transcriptome analysis was performed after 60 min when *B. subtilis* treated with 3 mM  $\text{Al}_2\text{O}_3$  NPs, using control cells and bulk- $\text{Al}_2\text{O}_3$  as references (see Fig. S4 assay and Table S1 assay for the overview of cellular processes regulated at the transcriptional level).

Two-component signal systems (TCS) are one means that bacteria have to respond to external stimuli. The transcriptome shows that the LiaRS TCS was involved in the adaptation to  $\text{Al}_2\text{O}_3$  NPs stress, as most of the related genes were highly upregulated (Fig. 4A). The response regulator/histidine kinase pair LiaRS of *Bacillus subtilis*, together with its membrane-bound inhibitor protein LiaF, constitutes an envelope stress sensing module that is conserved in *Firmicutes* bacteria<sup>21</sup>. LiaRS strongly responds to the presence of a number of cell wall antibiotics, such as bacitracin<sup>22</sup>. The exact physiological role of *LiaI* and *LiaH* is not well understood, but the proteins seem to be involved in sensing and counteracting membrane damage<sup>23</sup>. Additionally, genes in BceRS TCS, which mainly regulated the cell envelope stress response<sup>24,25</sup>, were also upregulated in the adaptation to  $\text{Al}_2\text{O}_3$  NP stress.

The membrane proteins are the integral part of the bacterial cell membrane to maintain the cell integrity. The transcriptome shows that many proteins integral to membrane were up-regulated, such as membrane protein OxaA, mechanosensitive channels. While inner membrane proteins involved in sporulation were down-regulated



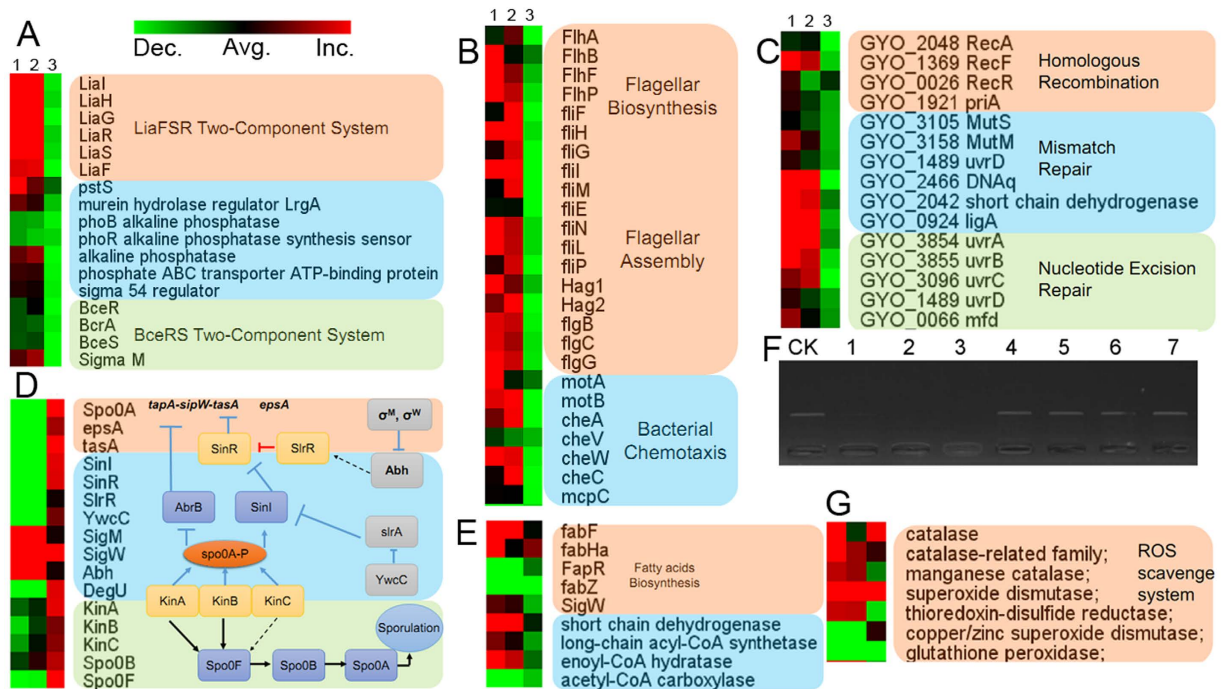


**Figure 4. Gene expression profiles for several representative categories.** Displayed are the relative expression levels of each gene. The numbers 1, 2, and 3 indicate  $\text{Al}_2\text{O}_3$  NPs/control,  $\text{Al}_2\text{O}_3$  NPs/bulk- $\text{Al}_2\text{O}_3$ , and  $\text{Al}_2\text{O}_3$ /control, respectively. Color indications are red for increased expression, green for decreased expression and black for unchanged expression. (A) LiaRS TCS- and BceRS TCS-related genes; (B) Flagellar biosynthesis- and assembly-related genes; (C) DNA repair-related genes; (D) Biofilm formation-related genes; (E) Fatty acids biosynthesis and metabolism genes; (F) Using plasmid pET42a for DNA damage detection *in vitro*. CK indicates control, 1 indicates UV treatment, 2 indicates 10 mM  $\text{Al}_2\text{O}_3$  NP treatment, 3 indicates 1 mM  $\text{Al}_2\text{O}_3$  NP treatment, 4 indicates 0.1 mM  $\text{Al}_2\text{O}_3$  NP treatment, 5 indicates 10 mM bulk- $\text{Al}_2\text{O}_3$  treatment, 6 indicates 1 mM bulk- $\text{Al}_2\text{O}_3$  treatment, 7 indicates 0.1 mM bulk- $\text{Al}_2\text{O}_3$  treatment; (G) ROS scavenger-related genes.

(Fig. S5). Taken together, these results indicate that membrane-related stress was one of the most important effects caused by  $\text{Al}_2\text{O}_3$  NPs.

**Fatty acids biosynthesis and lipid metabolism gene response to  $\text{Al}_2\text{O}_3$  NP stress.** The transcriptome showed that the genes related to fatty acid biosynthesis (*FabF*, *FabHa*) were upregulated in response to the  $\text{Al}_2\text{O}_3$  NPs stress (Fig. 4E), and *FapR*, involved in negative regulation of the fatty acid biosynthetic process<sup>26</sup>, was down-regulated (Fig. 4E). Increased abundance of the *FabF* elongation enzyme can increase the chain length of the resulting fatty acids<sup>27</sup>. Another key gene, extracytoplasmic function  $\sigma$  factor  $\sigma^W$ , was also induced (Fig. 4E), which was reported have a function in regulation of *FabHa* and *FabF*<sup>28</sup>. Additionally, expressions of some genes involved in the lipid metabolism were influenced by  $\text{Al}_2\text{O}_3$  NP stress (Fig. 4E). For example, long-chain acyl-CoA synthetase was induced, which was reported to activate fatty acids by thioesterification with coenzyme A. Fatty acyl-CoA molecules are then readily utilized for the biosynthesis of storage and membrane lipids<sup>29</sup>.

To test whether  $\text{Al}_2\text{O}_3$  NPs could affect the fatty acids profiles, fatty acid profiles of cultures after exposure to  $\text{Al}_2\text{O}_3$  NPs were analyzed and compared with the profiles of non-exposed cultures or cultures exposed to bulk-materials. Analysis revealed changes in membrane composition exclusively when cells were exposed to  $\text{Al}_2\text{O}_3$  NPs at a concentration of 3 mM but not in cultures exposed to bulk-material (Table 1). The major changes were observed in proportions of *i*- $\text{C}_{13:0}$ ,  $\text{C}_{15:0}$ , *i*- $\text{C}_{14:0}$ -3OH, and  $\text{C}_{18:0}$  (Table 1).

**Expression of genes involved in flagellar assembly and chemotaxis enhanced in the presence of  $\text{Al}_2\text{O}_3$  NPs.** The transcription of flagellar biosynthesis genes (e.g., *FlhA*, *FlhB*, *FlhF*, and *flgBCG*) were highly upregulated, as well as most of the flagellar assembly genes (e.g., *FliE-I*) (Fig. 4B). Most prominent among the upregulated genes are the large *flgB* operon and the *hag* gene, both involved in motility. Flagella are constructed from over 20 different proteins that must be assembled with the correct order and in the correct stoichiometry<sup>30</sup>.

To ensure proper assembly, flagellar gene expression is organized in at least two hierarchical levels defined here as “early-class” genes, recognized by  $\sigma^{70}$ , and “late-class” genes, recognized by the alternative sigma factor  $\sigma^{28/31}$ . *FliE*, encoding the flagellar hook-basal body complex protein, is a classic Early-class flagellar genes, was upregulated at the point of 60 min (Fig. 4B). *MotA* and *MotB*, encoding the protein components of the stator of proton-driven motors, were also upregulated (Fig. 4B). Generally, *FliM* secretion liberates its cognate  $\sigma^{28}$  to direct expression of the late-class flagellar genes. However, *FliM* was also upregulated at this time (Fig. 4B). Considering that  $\text{Al}_2\text{O}_3$  NPs could eliminate the flagella when flocculation occurred, the types of regulated genes indicated that

Peak Name <sup>a</sup>	CK	bulk-Al <sub>2</sub> O <sub>3</sub>	Al <sub>2</sub> O <sub>3</sub> NPs
%12:0 ISO	ND	0.92 ± 0.03	0.65 ± 0.03
%13:0 ISO	ND	ND	0.16 ± 0.02**
%13:0 ANTEISO	ND	0.68 ± 0.04	0.48 ± 0.11
%14:0 ISO	10.77 ± 0.15	11.93 ± 0.39	9.53 ± 0.27
%14:0	ND	0.85 ± 0.07	0.82 ± 0.04
%15:0 ISO	9.62 ± 0.08	9.43 ± 0.11	9.67 ± 0.09
%15:0 ANTEISO	34.86 ± 0.41	35.76 ± 0.98	34.26 ± 0.83
%15:0	ND	ND	0.29 ± 0.04**
%14:0 ISO 3OH	ND	ND	0.3 ± 0.07**
%16:0 ISO	20.41 ± 0.28	19.52 ± 0.74	19.5 ± 0.66
%16:0	8.55 ± 0.13	7.11 ± 0.11	7.94 ± 0.51
%17:0 ISO	6.9 ± 0.09	5.18 ± 0.17	6.32 ± 0.74
%17:0 ANTEISO	8.89 ± 0.11	6.96 ± 0.13	8.27 ± 0.28
%18:0 ISO	ND	0.54 ± 0.05	0.66 ± 0.06
%18:0	ND	0.53 ± 0.03	1.14 ± 0.09*

**Table 1. The effect of Al<sub>2</sub>O<sub>3</sub> NPs on membrane composition.** Data are presented as the average of three trials (± standard error, \*P ≤ 0.05, \*\*P). <sup>a</sup>Data derived from FAME analysis of the following treatment: CK indicates control, Al<sub>2</sub>O<sub>3</sub> NPs indicates 3 mM Al<sub>2</sub>O<sub>3</sub> NPs treated for 24 h, and bulk-Al<sub>2</sub>O<sub>3</sub> indicates 3 mM bulk-Al<sub>2</sub>O<sub>3</sub> treated for 24 h.

the flagella damage caused by Al<sub>2</sub>O<sub>3</sub> NPs occurred at different levels, and cells needed to express various genes belonging to different hierarchical levels to repair the flagellar system.

The transcriptomic data also show that many genes belonging to the chemotaxis system [e.g., chemoreceptor proteins (methylated chemotaxis proteins, MCPs), chemotaxis histidine kinase (CheA), and chemotaxis proteins (CheW and CheC)] are upregulated in the Al<sub>2</sub>O<sub>3</sub> NP treatment (Fig. 4B). The response of the MCPs is transmitted via the CheA histidine kinase that is complexed, together with adaptor protein CheW, on the cytoplasmic side<sup>32</sup>. In addition, other genes that improve the cell motility and secretion were also upregulated such as *ClpX* (encoding ATP-dependent Clp protease proteolytic subunit) (Fig. 4B).

**Al<sub>2</sub>O<sub>3</sub> NPs affect the biofilm- and sporulation-related genes.** Biofilm formation is a social behavior that generates favorable conditions for sustained survival in the natural environment<sup>33</sup>. Generally, regulatory pathways that control biofilm formation include the Spo0A pathway, the SlrR–SinR epigenetic switch system [the YwcC and SlrA pathway and the Abh-extracytoplasmic function (ECF) RNA polymerase  $\sigma$ -factors pathway], and the DegS–DegU two-component system. The relationship of the four pathways is shown in Fig. 4D. The transcriptome analysis showed that most genes related to the Spo0A pathway (e.g., *KinA-C* and *spo0A*) were down-regulated, as well as *tapA-sipW-tasA* and *SinR* (Fig. 4D). Spo0A is a central transcriptional regulator that controls the expression of more than 100 genes, including those necessary for biofilm matrix gene expression and sporulation, by controlling the activity of the master regulator SinR, a repressor of the *eps* and *tapA-sipW-tasA* operons<sup>34</sup>.

Another pathway mediated by the TetR-type transcriptional repressor (YwcC) was down-regulated<sup>35</sup>. When YwcC receives an as-yet-unknown signal, slrA is derepressed and the matrix genes are induced by SlrA-mediated inactivation of SinR<sup>35</sup>. Meanwhile, the Abh-ECF  $\sigma$  factors pathway also showed a response to Al<sub>2</sub>O<sub>3</sub> NP stress (Fig. 4D); the Abh protein regulates the transcription of *slrR*, further inactivates SinR and then induces the expression of matrix genes<sup>36</sup>. The transcription of *abh* is controlled by several extracytoplasmic function (ECF) RNA polymerase  $\sigma$ -factors, including  $\sigma^M$ ,  $\sigma^W$  and  $\sigma^{X36}$ . ECF  $\sigma$ -factors are activated by a variety of external stimuli, including cell wall stress and specific antibiotics<sup>37</sup>.

At the same time, genes involved sporulation (e.g., *KinA-C*, *spo0F*, *spo0B*, and *spo0A*) were also suppressed in the Al<sub>2</sub>O<sub>3</sub> NP treatment at 60 min. the percentage of sporulated cells was quantified, and the results showed that a high concentration of Al<sub>2</sub>O<sub>3</sub> NPs could suppress the formation of spores within 72 h (Fig. S6).

**Upregulation of DNA damage repair-associated genes.** Following Al<sub>2</sub>O<sub>3</sub> NP treatment for 60 min, three group of genes (homologous recombination, mismatch repair, and nucleotide excision repair) belonging to the DNA damage repair system were upregulated (Fig. 4C). For example, RecA, which is central to genome integrity and is important for strand exchange during homologous recombination, stabilizing stalled replication forks, and induction of the SOS transcriptional response to DNA damage<sup>38</sup>, was upregulated in the treatment. Meanwhile, genes encoding DNA mismatch repair and nucleotide excision repair proteins were also upregulated (Fig. 4C).

A plasmid-based *in vitro* DNA damage assay<sup>39</sup> was used to study the intrinsic potential of the Al<sub>2</sub>O<sub>3</sub> NPs to damage double-stranded DNA. The gel electrophoresis results for various treatments are shown in Fig. 4F. The positive control used in this study was a UV-treated plasmid, which was completely degraded and appeared as smeared. Severe DNA damage was observed for Al<sub>2</sub>O<sub>3</sub> NPs, which induced complete degradation of plasmid DNA (Fig. 4F). By contrast, bulk-Al<sub>2</sub>O<sub>3</sub> had no effect on DNA damage, appearing similar to the negative control. This might be one way to induce the DNA repair response *in vivo*, because a previous study had demonstrated

the attachment of Al<sub>2</sub>O<sub>3</sub> NPs to the surface of the cell membrane and also their presence inside the cells due to formation of irregular-shaped pits and perforation on the surfaces of bacterial cells<sup>40</sup>. Furthermore, Al<sub>2</sub>O<sub>3</sub> NPs also induced the ROS scavenge system response, as some of the catalase-related family genes and super oxide dismutase (SOD) were upregulated (Fig. 4G). The physiological analysis also showed that high concentrations of Al<sub>2</sub>O<sub>3</sub> NPs could induce ROS in cells compared with bulk-Al<sub>2</sub>O<sub>3</sub> treatment and controls (Fig. 4B) and also might result in DNA damage *in vivo*<sup>9</sup>. However, the exact mechanisms for DNA damage *in vivo* need further study.

**Systematic validation of transcriptome data using real-time PCR.** To validate the transcriptome data and systematically analyze the expression of key genes during treatment with Al<sub>2</sub>O<sub>3</sub> NPs and to further elucidate the mechanism of adaption of marine *Bacillus subtilis* C01 to Al<sub>2</sub>O<sub>3</sub> NP stress, eighteen key genes were selected on the basis of their possible role in two-component signal systems, membrane integrity, stress response, flagellar assembly, motility, biofilm formation, DNA repair, transcriptional regulation, and surfactin biosynthesis for real-time PCR analysis (Fig. S7). The real-time PCR used the control treatment and bulk-Al<sub>2</sub>O<sub>3</sub> treatment as references, separately. Meanwhile, we detected the gene transcripts at 60 min, 12 h, and 24 h after treatment with Al<sub>2</sub>O<sub>3</sub> NPs. The quantitative gene expression results correlated with the trend of regulation observed in the transcriptome experiment. In general, the relative expression of genes in Al<sub>2</sub>O<sub>3</sub> NPs/control were similar to those in Al<sub>2</sub>O<sub>3</sub> NPs/bulk-Al<sub>2</sub>O<sub>3</sub>, and the genes showed different responses to Al<sub>2</sub>O<sub>3</sub> NPs at different time points (Fig. S7). During the early stages of Al<sub>2</sub>O<sub>3</sub> NP stress, *LiaR*, as a key gene in LiaRS two-component signal systems mainly regulating the cell envelope stress response, was highly upregulated. Prolonged Al<sub>2</sub>O<sub>3</sub> NPs stress for 24 h leads to normal levels of *LiaR*. Genes involved in membrane integrity, SOD genes, and catalase genes were up-regulated last for a long time (last for 24 h). Genes involved in biosynthesis of flagellar components (*flgB* and *fliE*) exhibited a dramatic enhancement in their expression at 60 min after Al<sub>2</sub>O<sub>3</sub> NP treatment; however, these genes recovered to the normal level of expression for continued exposure to Al<sub>2</sub>O<sub>3</sub> NPs at 12 h and 24 h (Fig. S7). *RecA*, involved in DNA repair, was also highly induced in the early stage of Al<sub>2</sub>O<sub>3</sub> NP stress (60 min); however, in the middle stage, *RecA* showed a dramatically decreased level of expression and then recovered to normal levels during the prolonged Al<sub>2</sub>O<sub>3</sub> NP exposure for 24 h (Fig. S7).

Most of biofilm formation and sporulation-related genes (*DegS*, *SinR*, *KinA*, *Spo0A*, *tasA*, *epsA*, and *abrB*) were down-regulated in the early stages of Al<sub>2</sub>O<sub>3</sub> NP stress; however, most of these genes were upregulated with prolonged with Al<sub>2</sub>O<sub>3</sub> NP exposure at 12 h or 24 h. Interestingly, the expression of *SinR* showed sustained down-regulation. Among those genes, both *SinR* and *AbrB* could repress *tapA-sipW-tasA* and *epsA* expression. The prolonged stress leading to down-regulation of *SinR* might induce the expression of *tasA* and *epsA*, and the repression from *AbrB* to *tasA-epsA* might be inhibited by high expression of *spo0A* (Fig. S7), thereby inducing biofilm formation in shake cultures (Fig. 2A). However, the exact mechanisms need to be clarified in future studies.

More importantly, in this experiment, surfactin production was enhanced during the prolonged Al<sub>2</sub>O<sub>3</sub> NP stress for 60 h (Fig. 1C). However, the transcriptome showed the genes involved in the surfactin biosynthesis (*srfAA-D*) showed no significant change in expression, as even the regulation gene (*comA*) was down-regulated in the early stages (data not shown). The real-time PCR results showed that *comA* and *srfA* were indeed down-regulated during the early stages of stress but were induced with prolonged stress, and both were upregulated at 24 h; however, *comA* also showed down-regulation at 12 h treatment (Fig. S7). These results were consistent with the phenotypes in the former experiments (Fig. 2B).

## Discussion

Recently, it has been widely accepted that NPs can offer a new strategy to tackle multidrug-resistant bacteria<sup>41,42</sup>. Many studies have focused on the antibacterial properties of NPs, and described the toxicity mechanisms of NPs against bacteria and drug-resistant bacteria<sup>9,10</sup>. However, the few existing reports on the defense mechanisms of tolerant bacteria against NPs are limited to *Mycobacterium smegmatis* with Cu-doped TiO<sub>2</sub> NPs<sup>43</sup>, *B. subtilis* and *Pseudomonas putida* with nC<sub>60</sub><sup>44</sup>, and *Cupriavidus metallidurans* CH34 with Al<sub>2</sub>O<sub>3</sub> NPs<sup>45</sup> and do not provide mechanistic insights by using full transcriptional analysis. Whether secondary metabolism biosynthesis could respond to NP stress and enhance the adaption of bacteria to NPs was unknown.

The Al<sub>2</sub>O<sub>3</sub> NPs have been shown to attack the bacterial cell membrane, alter membrane permeability<sup>15,46</sup>, and even accumulate inside the bacterial cell<sup>40</sup>. In agreement with this report, in our study, Al<sub>2</sub>O<sub>3</sub> NPs could attach to the cell membrane, affect the cell morphology and even cause membrane damage (Fig. 3). Meanwhile, toxicity analysis showed that relatively high concentrations of Al<sub>2</sub>O<sub>3</sub> NPs could cause membrane damage compared with bulk-Al<sub>2</sub>O<sub>3</sub>. Further transcriptional analysis showed that at least 200 genes encoding proteins related to membrane components were regulated by Al<sub>2</sub>O<sub>3</sub> NPs at the early stage of stress (Fig. S4), including genes involved in the LiaRS TCS<sup>23</sup> and the BceRS TCS<sup>24,25</sup>, both of which were involved in sensing and counteracting membrane damage (Figs 4A and S7). Extracytoplasmic function (ECF) RNA polymerase  $\sigma$ -factors ( $\sigma^W$ ,  $\sigma^M$ ), involved in stress responses elicited by compounds that affect membrane integrity and/or fluidity, were also upregulated in the early stage of Al<sub>2</sub>O<sub>3</sub> NP stress. Cells have evolved the ability to modify membrane lipid composition to acclimatize to membrane stress<sup>28</sup>. In this sense, Kingston *et al.*<sup>28</sup> suggested that the  $\sigma^W$ -dependent stress response in *B. subtilis* could regulate the fatty acids biosynthesis and reduce the membrane fluidity. Accordingly, our results show that the genes involved in fatty acids biosynthesis and the fatty acid profiles were changed with Al<sub>2</sub>O<sub>3</sub> NP stress, and *i*-C<sub>13:0</sub>, C<sub>15:0</sub>, *i*-C<sub>14:0</sub>-3OH, and C<sub>18:0</sub> were induced, which contribute to antioxidant stress and improve the stability of the membrane<sup>28,47</sup>, however, the results were different to nC<sub>60</sub> treatment, under which *B. subtilis* showed an increase in membrane fluidity<sup>44</sup>. In this study, ROS generation was also induced in the early stage, which might be related to the membrane damage. In other bacteria, Al<sub>2</sub>O<sub>3</sub> NP was also found to cause the membrane damage

and induce the intracellular ROS in *E. coli* MG1655 and *Cupriavidus metallidurans* CH34<sup>45</sup>. Taken together, these results suggest that membrane-related stress was one of the most important effects caused by Al<sub>2</sub>O<sub>3</sub> NPs.

It was reported that some NPs such as Cu NPs<sup>9</sup> and Ag NPs<sup>48</sup> could damage DNA and cause growth inhibition of bacteria. However, whether Al<sub>2</sub>O<sub>3</sub> NPs have such properties remains unclear. In this study, the transcriptional analysis showed DNA damage repair-associated genes were highly upregulated in the early stage of Al<sub>2</sub>O<sub>3</sub> NP stress. Additionally, we found that a high concentration of Al<sub>2</sub>O<sub>3</sub> NPs could damage DNA *in vitro* (Fig. 4F). Furthermore, NPs generated ROS could cause DNA damage and induce DNA repair genes<sup>9</sup>. Coupled with the membrane damage and the induction of cellular ROS, Al<sub>2</sub>O<sub>3</sub> NPs probably induce the DNA damage *in vivo*. This result is in accordance with previously published data, which Cu NPs induce DNA damage in *E. coli*<sup>9</sup>, however, the exact mechanism for DNA damage needs further study.

Flagella enable *Bacillus subtilis* to move towards favorable environments or avoid harmful stimuli during swimming<sup>20</sup>. To avoid the stress of Al<sub>2</sub>O<sub>3</sub> NPs, *B. subtilis* had to regulate the expression of flagellar biosynthesis genes as well as most of the flagellar assembly genes (Fig. 4B). In this study, TEM analysis showed that Al<sub>2</sub>O<sub>3</sub> NPs could attach to the membrane and flagella, causing flagellar damage. As a result, *B. subtilis* upregulates the expression of the flagellar biosynthesis genes and flagellar assembly genes to repair the impaired flagella. Although the flagellar-related genes showed high expression following Al<sub>2</sub>O<sub>3</sub> NP treatment, the motility was not enhanced. This is probably because flagellar damage restricted the motility or the attachment of Al<sub>2</sub>O<sub>3</sub> NPs to cells increased the resistance to motility.

Swarming and sliding motility by *B. subtilis* were shown to require or be facilitated by the production of the lipopeptide surfactin<sup>20</sup>. In agreement with their report, our data showed that surfactin could restore and enhance swarming motility under Al<sub>2</sub>O<sub>3</sub> NP stress (Fig. 3). During Al<sub>2</sub>O<sub>3</sub> NP-treated fermentation, the induced surfactin production may alleviate the motility restriction to enhance chemotaxis in an attempt to eliminate the Al<sub>2</sub>O<sub>3</sub> NPs, as chemotaxis genes were also induced in this experiment. Interestingly, the surfactin produced could also reduce the surface tension<sup>49</sup>, which may help to wash Al<sub>2</sub>O<sub>3</sub> NPs away from cells. However, this needs to be determined in further studies.

Bacterial biofilms are multicellular communities in which cells are held together by an extracellular matrix to strengthen the adaption to various environmental factors<sup>50,51</sup>. In full agreement with these reports, our results showed a series of genes involved in biofilm formation were induced in different stages of Al<sub>2</sub>O<sub>3</sub> NP treatment. In the early stage, the YwcC–SlrA pathway and the Abh–ECF  $\sigma$  factors pathway were induced for a quick response to Al<sub>2</sub>O<sub>3</sub> NPs stress, while in the late stage, the spo0A pathway was activated and up-regulated *tasA* and *epsA* genes (Figs 4D and S7). Similar results were found in *Shewanella oneidensis* MR-1 response to Cu-doped TiO<sub>2</sub> NPs. *S. oneidensis* MR-1 could produce a large amount of extracellular polymeric substances (EPS) under NP stress, especially extracellular protein<sup>43</sup>. Surfactin, produced by constituent cells of the biofilm, was the first molecule identified as an inducer of matrix gene expression<sup>52</sup>. A recent study showed that surfactin could trigger the biofilm formation of *B. subtilis* in melon phylloplane<sup>51</sup>. The induction of surfactin in the late stage of Al<sub>2</sub>O<sub>3</sub> NP stress might contribute to the biofilm formation to alleviate Al<sub>2</sub>O<sub>3</sub> NP stress by separating *B. subtilis* from the Al<sub>2</sub>O<sub>3</sub> NPs (Fig. S8).

In summary, our transcriptome and physiological analyses suggest that the attachment of Al<sub>2</sub>O<sub>3</sub> NPs to the membrane of *B. subtilis* along with flagellar damage would initiate sensing and counteracting membrane damage. These responses also lead to changes in the membrane fatty acids profile, induction of DNA repair and the ROS scavenger system, and enhancement of flagellar biosynthesis to repair the organism, resulting in optimal conditions for *B. subtilis* growth and adaptation to Al<sub>2</sub>O<sub>3</sub> NPs in the early stage of stress. Furthermore, biofilm formation and surfactin biosynthesis were induced in the late stage to adapt to or avoid the stress (Fig. S8).

## Methods

**Strains and culture conditions.** Marine *Bacillus sp.* strain C01, isolated from Weihai, was grown at 30 °C in Landy medium<sup>16</sup>. A 1% inoculum volume of culture was used to inoculate a 250 mL flask containing 100 ml of Landy medium, which was incubated for 72 h on an orbital shaker (150 rpm) at 30 °C. Al<sub>2</sub>O<sub>3</sub> NPs were added as an inductor at different times.

**Preparation of Al<sub>2</sub>O<sub>3</sub> NPs and bulk-Al<sub>2</sub>O<sub>3</sub> suspensions.** Al<sub>2</sub>O<sub>3</sub> NPs and bulk-Al<sub>2</sub>O<sub>3</sub> were purchased from Shenzhen Crystal Material Chemical Co., Ltd (Shenzhen, China). The suspensions of Al<sub>2</sub>O<sub>3</sub> NPs and bulk-Al<sub>2</sub>O<sub>3</sub> were diluted with ultra-pure water. To avoid aggregation, the suspensions were ultra-sonicated for 15 min in sealed sterile tubes before addition to the cell culture. The following concentrations were used in the experiment: 0, 0.3, 1, 3, and 10 mmol/L. The size of Al<sub>2</sub>O<sub>3</sub> NPs were detected by using Scanning Electron Microscope (Nova NanoSEM 450)<sup>15</sup>.

**Isolation of surfactin.** Crude surfactin was isolated by adding concentrated hydrochloric acid to the Landy media after removing the biomass by centrifugation. A precipitate was formed at pH 2 which could be collected, dried, and extracted with dichloromethane. The solvent was removed under reduced pressure to give an off-white solid. Further purification was achieved by recrystallization. The dichloromethane extract was dissolved in distilled water containing sufficient NaOH to produce a pH of 8. This solution was filtered and titrated to pH 2 with concentrated HCl. The white solid was collected as a pellet after centrifugation.

**Quantitative analysis of surfactin by HPLC.** The isolated surfactin was dissolved in 1 mL of methanol followed by charcoal treatment and passed through a 0.22-  $\mu$ m-pore filter. The filtrate was subjected to HPLC on a reversed-phase column (RP-C18, 5  $\mu$ m, 4\*250 mm; Merck). The column was eluted at a flow rate of 1.0 mL/min with acetonitrile-water (80:20, v/v) and monitored at 214 nm. The concentration of surfactin was determined with a calibration curve made with authentic surfactin purchased from Sigma (S3523).



**Quantitative analysis of biofilm formation.** At specific times, planktonic cells were removed, biofilm cells were stained with 2 ml of 0.3% crystal violet for 10 min, washed with distilled water, and air dried. The crystal violet in the biofilm cells was solubilized with 2 ml of 70% ethanol, and the optical density at 570 nm (OD<sub>570</sub>) was measured<sup>53</sup>.

**Cell morphology and motility study.** The effect of Al<sub>2</sub>O<sub>3</sub> NPs on *Bacillus* cell morphology and the attachment of Al<sub>2</sub>O<sub>3</sub> NPs to *B. subtilis* were studied using transmission electron microscopy (TEM)<sup>15</sup>.

Bacterial motility over a surface was analyzed by spotting 2 µl culture of each strain grown overnight (~10<sup>5</sup> cells) onto the center of soft agar plates (2216E media with 0.3% agar) with different treatments. Plates were incubated at 30 °C in a humidified chamber for 6–8 h.

## References

- Oberdorster, G., Oberdorster, E. & Oberdorster, J. Nanotoxicology: an emerging discipline evolving from studies of ultrafine particles. *Environmental health perspectives* **113**, 823–839 (2005).
- Farokhzad, O. C. *et al.* Targeted nanoparticle-aptamer bioconjugates for cancer chemotherapy *in vivo*. *Proceedings of the National Academy of Sciences of the United States of America* **103**, 6315–6320, doi: 10.1073/pnas.0601755103 (2006).
- Shrivastava, S. *et al.* Characterization of enhanced antibacterial effects of novel silver nanoparticles. *Nanotechnology* **18**, doi: 10.1088/0957-4484/18/22/225103 (2007).
- Neal, A. L. What can be inferred from bacterium-nanoparticle interactions about the potential consequences of environmental exposure to nanoparticles? *Ecotoxicology* **17**, 362–371, doi: 10.1007/s10646-008-0217-x (2008).
- Huh, A. J. & Kwon, Y. J. “Nanoantibiotics”: A new paradigm for treating infectious diseases using nanomaterials in the antibiotics resistant era. *J Control Release* **156**, 128–145, doi: 10.1016/j.jconrel.2011.07.002 (2011).
- Hajipour, M. J. *et al.* Antibacterial properties of nanoparticles. *Trends in biotechnology* **30**, 499–511, doi: 10.1016/j.tibtech.2012.06.004 (2012).
- Kaweeteerawat, C. *et al.* Toxicity of Metal Oxide Nanoparticles in *Escherichia coli* Correlates with Conduction Band and Hydration Energies. *Environmental science & technology* **49**, 1105–1112, doi: 10.1021/es504259s (2015).
- Friedman, A. *et al.* Susceptibility of Gram-positive and -negative bacteria to novel nitric oxide-releasing nanoparticle technology. *Virulence* **2**, 217–221 (2011).
- Kaweeteerawat, C. *et al.* Cu Nanoparticles Have Different Impacts in *Escherichia coli* and *Lactobacillus brevis* than Their Microsized and Ionic Analogues. *ACS nano* **9**, 7215–7225, doi: 10.1021/acsnano.5b02021 (2015).
- McQuillan, J. S. & Shaw, A. M. Differential gene regulation in the Ag nanoparticle and Ag(+)-induced silver stress response in *Escherichia coli*: a full transcriptomic profile. *Nanotoxicology* **8**, Suppl 1, 177–184, doi: 10.3109/17435390.2013.870243 (2014).
- Kaweeteerawat, C. *et al.* Toxicity of metal oxide nanoparticles in *Escherichia coli* correlates with conduction band and hydration energies. *Environ Sci Technol* **49**, 1105–1112, doi: 10.1021/es504259s (2015).
- Pakrashi, S. *et al.* Cytotoxicity of Al<sub>2</sub>O<sub>3</sub> Nanoparticles at Low Exposure Levels to a Freshwater Bacterial Isolate. *Chem Res Toxicol* **24**, 1899–1904, doi: 10.1021/Tx200244g (2011).
- Sinha, R., Karan, R., Sinha, A. & Khare, S. K. Interaction and nanotoxic effect of ZnO and Ag nanoparticles on mesophilic and halophilic bacterial cells. *Bioresour Technol* **102**, 1516–1520, doi: 10.1016/j.biortech.2010.07.117 (2011).
- Qiu, Z. *et al.* Nanoalumina promotes the horizontal transfer of multiresistance genes mediated by plasmids across genera. *Proceedings of the National Academy of Sciences of the United States of America* **109**, 4944–4949, doi: 10.1073/pnas.1107254109 (2012).
- Jiang, W., Mashayekhi, H. & Xing, B. Bacterial toxicity comparison between nano- and micro-scaled oxide particles. *Environmental pollution* **157**, 1619–1625, doi: 10.1016/j.envpol.2008.12.025 (2009).
- Mu, D., Mu, X., Xu, Z., Du, Z. & Chen, G. Removing *Bacillus subtilis* from fermentation broth using alumina nanoparticles. *Bioresour Technol* **197**, 508–511, doi: 10.1016/j.biortech.2015.08.109 (2015).
- Shapiro, J. Bacteria as multicellular organisms. *Scientific Am* **258**, 82 (1988).
- Aguilar, C., Vlamakis, H., Losick, R. & Kolter, R. Thinking about *Bacillus subtilis* as a multicellular organism. *Curr Opin Microbiol* **10**, 638–643, doi: 10.1016/j.mib.2007.09.006 (2007).
- Kearns, D. B. A field guide to bacterial swarming motility. *Nat Rev Microbiol* **8**, 634–644, doi: 10.1038/nrmicro2405 (2010).
- Ghelardi, E. *et al.* Contribution of surfactin and SwrA to flagellin expression, swimming, and surface motility in *Bacillus subtilis*. *Appl Environ Microbiol* **78**, 6540–6544, doi: 10.1128/AEM.01341-12 (2012).
- Schrecke, K., Jordan, S. & Mascher, T. Stoichiometry and perturbation studies of the LiaFSR system of *Bacillus subtilis*. *Mol Microbiol* **87**, 769–788, doi: 10.1111/mmi.12130 (2013).
- Kesel, S., Mader, A., Hofler, C., Mascher, T. & Leisner, M. Immediate and heterogeneous response of the LiaFSR two-component system of *Bacillus subtilis* to the peptide antibiotic bacitracin. *PLoS one* **8**, e53457, doi: 10.1371/journal.pone.0053457 (2013).
- Wolf, D. *et al.* In-depth profiling of the LiaR response of *Bacillus subtilis*. *J Bacteriol* **192**, 4680–4693, doi: 10.1128/JB.00543-10 (2010).
- Ouyang, J., Tian, X. L., Versey, J., Wishart, A. & Li, Y. H. The BceABRS four-component system regulates the bacitracin-induced cell envelope stress response in *Streptococcus mutans*. *Antimicrob Agents Chemother* **54**, 3895–3906, doi: 10.1128/AAC.01802-09 (2010).
- Ohki, R. *et al.* The BceRS two-component regulatory system induces expression of the bacitracin transporter, BceAB, in *Bacillus subtilis*. *Mol Microbiol* **49**, 1135–1144 (2003).
- Wenzel, M. *et al.* Proteomic signature of fatty acid biosynthesis inhibition available for *in vivo* mechanism-of-action studies. *Antimicrob Agents Chemother* **55**, 2590–2596, doi: 10.1128/AAC.00078-11 (2011).
- Schujman, G. E. & de Mendoza, D. Regulation of type II fatty acid synthase in Gram-positive bacteria. *Current Opinion in Microbiology* **11**, 148–152, doi: 10.1016/j.mib.2008.02.002 (2008).
- Kingston, A. W., Subramanian, C., Rock, C. O. & Helmann, J. D. A sigmaW-dependent stress response in *Bacillus subtilis* that reduces membrane fluidity. *Mol Microbiol* **81**, 69–79, doi: 10.1111/j.1365-2958.2011.07679.x (2011).
- Fullekrug, J. & Poppelreuther, M. Measurement of Long-Chain Fatty Acyl-CoA Synthetase Activity. *Methods Mol Biol* **1376**, 43–53, doi: 10.1007/978-1-4939-3170-5\_5 (2016).
- Fujinami, S., Terahara, N., Krulwich, T. A. & Ito, M. Motility and chemotaxis in alkaliphilic *Bacillus* species. *Future Microbiol* **4**, 1137–1149, doi: 10.2217/fmb.09.76 (2009).
- Chevanne, F. F. & Hughes, K. T. Coordinating assembly of a bacterial macromolecular machine. *Nat Rev Microbiol* **6**, 455–465, doi: 10.1038/nrmicro1887 (2008).
- Lamanna, A. C., Ordal, G. W. & Kiessling, L. L. Large increases in attractant concentration disrupt the polar localization of bacterial chemoreceptors. *Mol Microbiol* **57**, 774–785, doi: 10.1111/j.1365-2958.2005.04728.x (2005).
- Cairns, L. S., Hobley, L. & Stanley-Wall, N. R. Biofilm formation by *Bacillus subtilis*: new insights into regulatory strategies and assembly mechanisms. *Mol Microbiol* **93**, 587–598, doi: 10.1111/mmi.12697 (2014).
- Molle, V. *et al.* The Spo0A regulon of *Bacillus subtilis*. *Mol Microbiol* **50**, 1683–1701 (2003).

35. Chai, Y., Kolter, R. & Losick, R. Paralogous antirepressors acting on the master regulator for biofilm formation in *Bacillus subtilis*. *Mol Microbiol* **74**, 876–887, doi: 10.1111/j.1365-2958.2009.06900.x (2009).
36. Murray, E. J., Strauch, M. A. & Stanley-Wall, N. R. SigmaX is involved in controlling *Bacillus subtilis* biofilm architecture through the AbrB homologue Abh. *J Bacteriol* **191**, 6822–6832, doi: 10.1128/JB.00618-09 (2009).
37. Mascher, T. Signaling diversity and evolution of extracytoplasmic function (ECF) sigma factors. *Curr Opin Microbiol* **16**, 148–155, doi: 10.1016/j.mib.2013.02.001 (2013).
38. Cox, M. M. Regulation of bacterial RecA protein function. *Crit Rev Biochem Mol Biol* **42**, 41–63, doi: 10.1080/10409230701260258 (2007).
39. Leba, L. J. *et al.* Optimization of a DNA Nicking Assay to Evaluate *Oenocarpus bataua* and *Camellia sinensis* Antioxidant Capacity. *Int J Mol Sci* **15**, 18023–18039, doi: 10.3390/ijms151018023 (2014).
40. Ansari, M. A. *et al.* Interaction of Al<sub>2</sub>O<sub>3</sub> nanoparticles with *Escherichia coli* and their cell envelope biomolecules. *J Appl Microbiol* **116**, 772–783, doi: 10.1111/jam.12423 (2014).
41. Leid, J. G. *et al.* *In vitro* antimicrobial studies of silver carbene complexes: activity of free and nanoparticle carbene formulations against clinical isolates of pathogenic bacteria. *J Antimicrob Chemother* **67**, 138–148, doi: 10.1093/jac/dkr408 (2012).
42. Whitesides, G. M. Nanoscience, nanotechnology, and chemistry. *Small* **1**, 172–179, doi: 10.1002/sml.200400130 (2005).
43. Wu, B. *et al.* Bacterial responses to Cu-doped TiO<sub>2</sub> nanoparticles. *Sci Total Environ* **408**, 1755–1758, doi: 10.1016/j.scitotenv.2009.11.004 (2010).
44. Fang, J. S., Lyon, D. Y., Wiesner, M. R., Dong, J. P. & Alvarez, P. J. J. Effect of a fullerene water suspension on bacterial phospholipids and membrane phase behavior. *Environmental Science & Technology* **41**, 2636–2642, doi: 10.1021/es062181w (2007).
45. Simon-Deckers, A. *et al.* Size-, Composition- and Shape-Dependent Toxicological Impact of Metal Oxide Nanoparticles and Carbon Nanotubes toward Bacteria. *Environmental Science & Technology* **43**, 8423–8429, doi: 10.1021/es9016975 (2009).
46. Jiang, W., Ghosh, S., Song, L., Vachet, R. W. & Xing, B. S. Effect of Al<sub>2</sub>O<sub>3</sub> nanoparticles on bacterial membrane amphiphilic biomolecules. *Colloid Surface B* **102**, 292–299, doi: 10.1016/j.colsurfb.2012.08.043 (2013).
47. Vodovnik, M., Kostanjsek, R., Zorec, M. & Logar, R. M. Exposure to Al<sub>2</sub>O<sub>3</sub> nanoparticles changes the fatty acid profile of the anaerobe *Ruminococcus flavefaciens*. *Folia Microbiol* **57**, 363–365, doi: 10.1007/s12223-012-0143-4 (2012).
48. Juan, L., Zhimin, Z., Anchun, M., Lei, L. & Jingchao, Z. Deposition of silver nanoparticles on titanium surface for antibacterial effect. *Int J Nanomedicine* **5**, 261–267 (2010).
49. Angelini, T. E., Roper, M., Kolter, R., Weitz, D. A. & Brenner, M. P. *Bacillus subtilis* spreads by surfing on waves of surfactant. *Proc Natl Acad Sci USA* **106**, 18109–18113, doi: 10.1073/pnas.0905890106 (2009).
50. Romero, D., Aguilar, C., Losick, R. & Kolter, R. Amyloid fibers provide structural integrity to *Bacillus subtilis* biofilms. *Proc Natl Acad Sci USA* **107**, 2230–2234, doi: 10.1073/pnas.0910560107 (2010).
51. Zeriuoh, H., de Vicente, A., Perez-Garcia, A. & Romero, D. Surfactin triggers biofilm formation of *Bacillus subtilis* in melon phylloplane and contributes to the biocontrol activity. *Environmental microbiology* **16**, 2196–2211, doi: 10.1111/1462-2920.12271 (2014).
52. Lopez, D., Fischbach, M. A., Chu, F., Losick, R. & Kolter, R. Structurally diverse natural products that cause potassium leakage trigger multicellularity in *Bacillus subtilis*. *P Natl Acad Sci USA* **106**, 280–285, doi: 10.1073/pnas.0810940106 (2009).
53. Hsueh, Y. H., Somers, E. B., Lereclus, D. & Wong, A. C. L. Biofilm formation by *Bacillus cereus* is influenced by PlcR, a pleiotropic regulator. *Appl Environ Microb* **72**, 5089–5092, doi: 10.1128/Aem.00573-06 (2006).

## Acknowledgements

This work was supported by the National Natural Science Foundation of China (Project No. 31400102), the Postdoctoral Science Foundation of China (Project No. 2015M570587), Marine Research Institute Foundation of Shandong University and City of Weihai (Project No. 2014DXGJ38), and a grant from key lab of marine bioactive substance and modern analytical technique, State Oceanic Administration, China (MBSMAT-2013-03).

## Author Contributions

D.M., Z.D. and G.C. designed the study and wrote the manuscript. D.M. and X.Y. did the physiological analyses. D.M. and Z.X. performed the transcriptome sequencing. D.M. analyzed the data of the transcriptome. Z.D. and G.C. discussed the results and commented on the paper.

## Additional Information

**Supplementary information** accompanies this paper at <http://www.nature.com/srep>

**Competing financial interests:** The authors declare no competing financial interests.

**How to cite this article:** Mu, D. *et al.* Physiological and transcriptomic analyses reveal mechanistic insight into the adaptation of marine *Bacillus subtilis* C01 to alumina nanoparticles. *Sci. Rep.* **6**, 29953; doi: 10.1038/srep29953 (2016).



This work is licensed under a Creative Commons Attribution 4.0 International License. The images or other third party material in this article are included in the article's Creative Commons license, unless indicated otherwise in the credit line; if the material is not included under the Creative Commons license, users will need to obtain permission from the license holder to reproduce the material. To view a copy of this license, visit <http://creativecommons.org/licenses/by/4.0/>